Chapter 2
Measurement of 3D Deformation Field of ECM Generated by Mesenchymal Stem Cell Using DVC Method

Yasuyuki Morita, Naoki Kawase, Takashi Yamauchi, and Yang Ju

Abstract Cells maintain homeostasis and express various functions by interacting mechanically with cell-adhesive matrix. As regarding cellular differentiation, it has been found that elasticity of the matrix determines differentiation lineage of mesenchymal stem cells (MSCs). The direct quantitative measurement of the mechanical interaction between MSC and matrix for differentiation, however, has not been performed. In the present work, the displacement field of the cell-adhesive matrix was observed quantitatively using digital volume correlation (DVC) method. In practice, the cellular traction stress was analyzed when the MSC differentiated into neuron or osteoblast on the soft or hard elastic matrix, respectively. Then, function of non-muscle myosin II (NMM II), which plays an important role in intracellular cytoskeletal dynamics, was investigated in cellular differentiation. As a result, the mechanical interaction between the cell and the matrix was dependent upon the elasticity of the matrix. Additionally, it has been shown that mechanical interaction between intracellular cytoskeleton and cell-adhesion matrix is indispensable for cellular differentiation.

Keywords Digital volume correlation (DVC) • Elastic modulus • Mesenchymal stem cell (MSC) • Differentiation • Extracellular matrix (ECM)

2.1 Introduction

MSC (Mesenchymal Stem Cell or Multipotent Stromal Cell) has self-renewal ability and plasticity. The MSCs can differentiate into wide variety of cells such as osteoblasts, chondrocytes, adipocytes, myocytes, cardiomyocytes, neurons etc [1–3]. They must have great promise with respect to stable supply of various mature cells in regenerative medicine since they are harvested relatively easily from bone marrow. Therefore, control technique of the stem cell differentiation is indispensable from the view point of steady cell supply. Mechanical stimulus [4–8] would be one of the prospective technologies for controlling differentiation because it is simple and easy although diverse technologies such as chemical factor [9], electrical and magnetic stimulus [10], and co-culture system [11, 12] have been developed. It has been becoming increasingly clearer that cell differentiation has a close relationship with mechanical microenvironment of extracellular matrix (ECM) around the cell [13, 14]. Engler et al. elucidated that only elasticity of cell-adhesive matrix was able to determine cellular differentiation lineage [15]. This knowledge is one of the crucial achievements to carry forward cell-differentiation controls due to mechanical microenvironment. However, there have been no reports to bring out in terms of mechanical interaction between cell and ECM with different matrix elasticity.

In the present work differentiation lineage of human bone marrow MSCs (hBMSCs) and three dimensional displacement field of cell-adhesive matrix produced by a hBMSC were evaluated quantitatively when the hBMSC was cultured on the two kinds of considerably different elasticity $E = 0.5$ kPa (soft) and 37 kPa (hard) in the cell-adhesive matrix. The differentiation assessment was performed by two ways morphological and gene expression evaluations. The 3D displacement field was analyzed by a digital volume correlation (DVC) method [16] using a confocal laser scanning microscope (CLSM) (FN1CSU; Nikon Instech). The 3D–traction stress of the cell was also obtained quantitatively. Furthermore the same evaluations the differentiation assessments and the gene expression levels were performed if intracellular non-muscle myosin II (NMM II) which plays an important role in cytoskeletal dynamics inside cell [17] was inhibited.

Y. Morita (✉) • N. Kawase • T. Yamauchi • Y. Ju
Department of Mechanical Science & Engineering, Graduate School of Engineering, Nagoya University, Furo-cho, Chikusa-ku, Nagoya, 464-8603, Japan
e-mail: morita@mech.nagoya-u.ac.jp

© The Society for Experimental Mechanics, Inc. 2018

P. Zavattieri et al. (eds.), *Mechanics of Biological Systems, Materials and other topics in Experimental and Applied Mechanics, Volume 4*, Conference Proceedings of the Society for Experimental Mechanics Series, DOI 10.1007/978-3-319-63552-1_2

2.2 Materials and Methods

2.2.1 Cell Culture

HBMSCs (UE6E7T-3; Riken Cell Bank) were maintained in low-glucose Dulbecco's modified Eagle's medium (DMEM; Wako Pure Chemical Industries, Ltd.) containing 10% fetal calf serum (Invitrogen) and 0.05% gentamicin (Invitrogen) at 37 °C under an atmosphere of 5% CO_2 in a humidified incubator. At near-confluence, which occurred every 5–7 days, the cells were detached from 25 cm^2 culture flasks (BD Biosciences) with 0.25 w/v% Trypsin-1 mM EDTA (Wako Pure Chemical Industries, Ltd.). Actin-GFP (Molecular Probes) was added into the suspension of the hBMSCs to stain the intracellular actin filaments for cellular morphology observation. Then, the cells were seeded onto polyacrylamide gel whose surface covered with a cellular adhesion molecule, human fibronectin (FN; Corning Incorporated Life Sciences), as described in the following sections.

2.2.2 Preparation of Polyacrylamide-Matrix Gel

Solutions of acrylamide (10 w/v%; Kanto Chemical Co., Inc., Tokyo, Japan) and N, N-methylene-bis-acrylamide (BIS; Kanto, Chemical Co., Inc.) were mixed with distilled water to fabricate the polyacrylamide. The blending quantity of BIS was 0.003 and 0.07 w/v% to change elasticity of the polyacrylamide. For measurement of 3D-displacement field by DVC method, fluorescent micro-particles (1.0-μm diameter, Molecular Probes) suspension was added to the polyacrylamide solution with 10 w/v% ammonium persulfate (Kanto, Chemical Co., Inc.) and TEMED (Amresco) which work as polymerization initiator and accelerator, respectively, in a volume ratio of 100 (polyacrylamide): 9 (micro-particles): 1 (ammonium persulfate): 1 (TEMED). 6 μl of the acrylamide solution was pipetted on the surface of a glass based dish which coated with aminosilane (Iwaki). Then, a cover glass (10-mm diameter, Matsunami Glass) was put onto the solution to make the top surface flat. Polymerization was allowed to proceed at room temperature for 5 min. Then, the polyacrylamide-matrix gel was thoroughly rinsed with distilled water. The typical geometry of the matrix was approximately 10 and 80 μm in diameter and thickness, respectively. The two kinds of elastic moduli of the polyacrylamide gel contained BIS of 0.003 or 0.07 w/v%, were 0.5 or 37 kPa, respectively. The elastic modulus of the matrix was determined by the penetration method [18].

2.2.3 Coating of the Polyacrylamide Matrix with Human Fibronectin

The human fibronectin was conjugated to the top surface of the acrylamide matrix using hetero-bifunctional crosslinker, sulfo-SANPAH (Terumo), to promote cell attachment to the polyacrylamide matrix. The typical thickness of the fibronectin layer was approximately 1 μm as determined by CLSM.

2.2.4 Cell Seeding and Differentiation Evaluation

The hBMSCs were seeded onto the matrix with low density of 1.6×10^4 cells, and cultured for 24 h. Two kinds of evaluation techniques for cellular differentiation, morphological assessment and gene expression analysis, were employed. In the morphological assessment, parameters of branches B and roundness R were adopted for evaluation of neurogenic and osteogenic differentiation, respectively. Meanwhile, enolase 2 (Eno2) and runt-related transcription factor 2 (Runx2) gene expression levels were analyzed using quantitative reverse transcription polymerase chain reaction (qRT-PCR) for the another differentiation evaluation, respectively. Eno2, commonly included in axon processes of neurons, is one of the specific enzymes of glycolysis [19]. Runx2 is an essential transcription factor for osteogenic differentiation [20]. Figure 2.1 shows the experimental arrangement in this study.

2.2.5 DVC Measurement and Calculation of Displacements, Strains, and Stresses

The full field 3D displacements of the polyacrylamide matrix were determined using CLSM and DVC method [21]. The DVC algorithm was referred to Ref. 16. In brief, confocal volume images of cell-seeded polyacrylamide matrix with randomly dispersed fluorescent particles were obtained after 24 h which the hBMSCs were seeded onto the matrix. The acquired

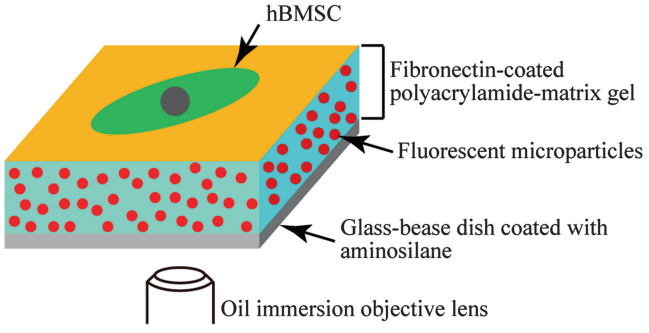


Fig. 2.1 Experimental arrangement. Fluorescent microparticles (1.0 μm diameter) were spread inside polyacrylamide-matrix gel for 3D displacement measurement by DVC. The typical geometry of the matrix was approximately 10 mm and 80 μm in diameter and thickness, respectively. Human fibronectin (approximately 1 μm thickness) was coated on the top surface of the matrix. HBMSCs were seeded onto the matrix at a density of 2.0×10^2 cells/mm^2. 3D confocal image stacks were acquired by CLSM that captured the emission from the fluorescent microparticles

volume of the matrix was $300 \times 300 \times 50$ μm^3, corresponding with $512 \times 512 \times 167$ voxels. Then, the confocal volume images were also obtained at the same position after 15 min. The stacked images were divided into a set of subvolumes that were centered on an area of interest. The local displacement vector can be obtained using a pair of corresponding subvolumes images through a three-dimensional volume correlation method. This was performed mathematically by representing the intensity patterns of each subvolume by two intensity functions $f(\boldsymbol{x})$ and $g(\boldsymbol{x})$ that have been translated relative to one another by a displacement vector $\boldsymbol{c}$ of each subset within the confocal volume image can be calculated through the cross-correlation of the two subset intensity functions [22]. The DVC algorithm programmed in this study was achieved displacement sensitivity of 41 nm with the CLMS. Finally, from the result of the 3D displacement field, traction stress of the cell was calculated along the top surface of the matrix, directly beneath the cell using the known Cauchy relationship: $\boldsymbol{T} = \sigma\, \boldsymbol{n}$, where $\boldsymbol{T}$ is the 3D surface traction stress vector, σ is the material stress tensor, and $\boldsymbol{n}$ is the surface normal. The complete mathematical details for determination of the traction stress can be found in Ref. 23.

2.2.6 NMM II Inhibition

As the final experiment, intracellular non-muscle myosin II (NMM II), which is likely to be involved in exerting force through focal adhesions in mechanisms of sensing matrix elasticity [15], was inhibited by blebbistantin (Sigma-Aldrich). The blebbistantin was added with the concentration of 50 μM after 6 h following the cells were seeded onto the polyacrylamide matrix.

2.2.7 Statistical Analysis

The number of samples, n, was indicated in each figure. The paired Student's t test was used for statistical analyses, and p values <0.01 and 0.05 were taken to indicate statistical significance.

2.3 Results and Discussion

The results of the cells without NMM II inhibitor whose data are plotted in red of Figs. 2.2 and 2.4, have been focused on initially. Figure 2.2a shows the morphological analysis for cellular differentiation with the elastic modulus of the polyacrylamide matrix. The cellular morphology was dependent upon the elastic modulus. There were also big differences with respect to the mRNA expression levels of Eno2 and Runx2 in the two kinds of elastic modulus of the matrix as shown in Fig. 2.2b. Namely, the maximum value of the expression levels for each marker, Eno2 and Runx2, was obtained on the matrix of $E = 0.5$ and 37 kPa, respectively. These results indicate that the differentiation of hBMSCs was dependent upon

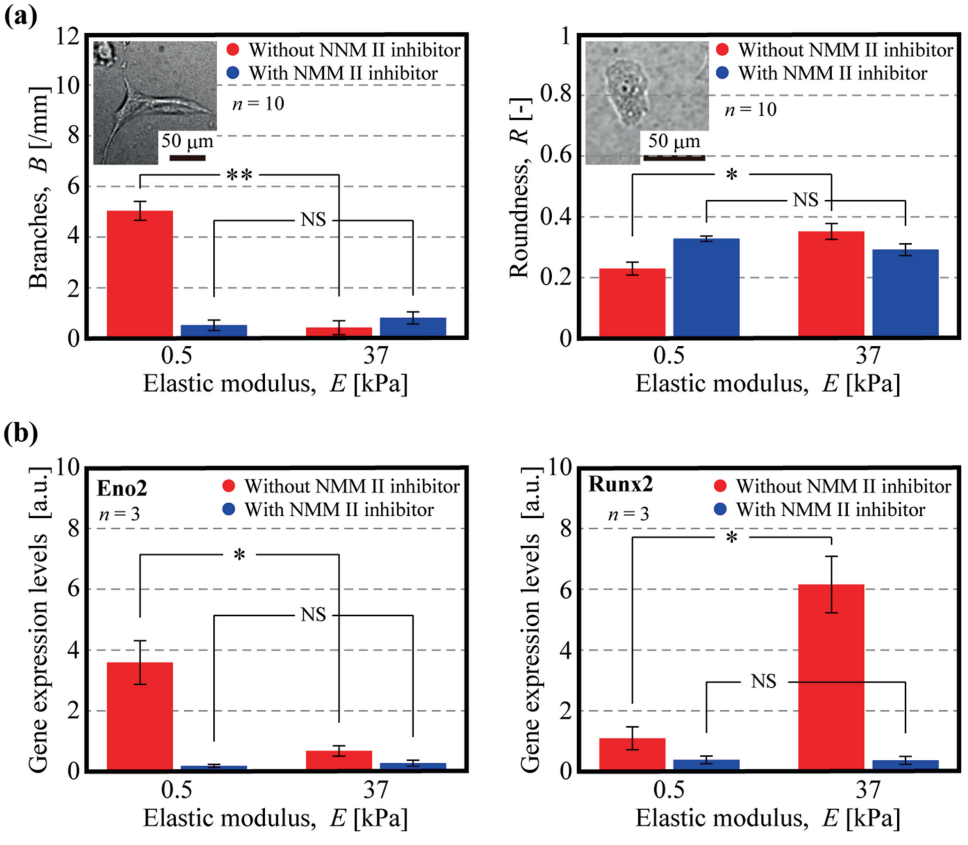


Fig. 2.2 Evaluation of differentiation of hBMSCs with elastic mudululs of polyacrylamide matrix. (**a**) Morphological analysis. Branches (*left*), roundness (*right*). *Inset* indicates the representative phase-contrast cell image at the maximum value without NMM II inhibitor. (**b**) mRNA expression levels. Eno2 for neurons (*left*), Runx2 for osteoblasts (*right*). *Red* and *blue* data represent without and with NMM II inhibitor, respectively. *n* indicates the number of samples. All data are indicated by Mean ± SEM. $^{**}p < 0.01$, $^{*}p < 0.05$. NS = not significant

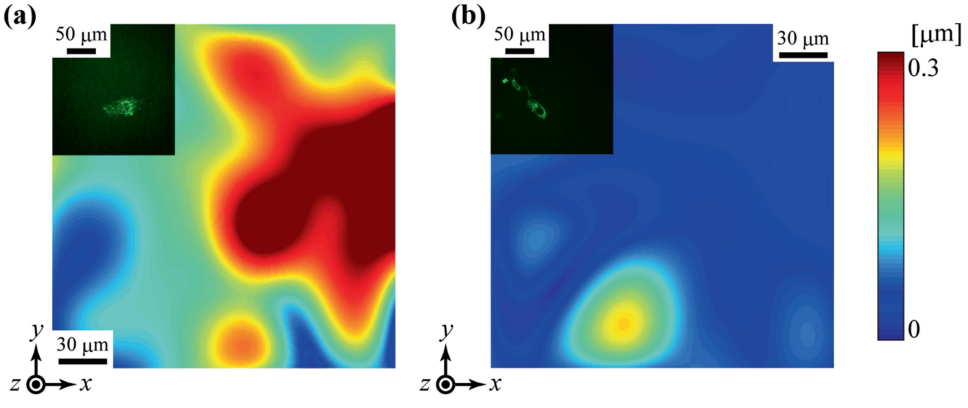


Fig. 2.3 Absolute displacement field of polyacrylamide matrix generated by cell without NMM II inhibitor. (**a**) Elastic modulus $E = 0.5$ kPa. (**b**) $E = 37$ kPa. Figures indicate the displacement field on the matrix. Inset indicates confocal fluorescence micrographs of the cell

the elasticity of the polyacrylamide matrix, and they underwent differentiation into neurons on $E = 0.5$ kPa, and osteoblasts on $E = 37$ kPa, respectively. This differentiation lineage agreed well with the findings of Engler et al. [15]. The displacement field generated by the cell on each elastic modulus of the matrix was shown in Fig. 2.3. The displacement denotes the absolute displacement. It suggests that a hBMSC produced large deformation (high displacement and wide area) to the matrix and differentiated into a neuron if the matrix was relatively soft. In contrast, it indicates that a hBMSC made small deformation (low displacement and narrow area) to the gel substrate and differentiated into a osteoblasts if the matrix was relatively hard.

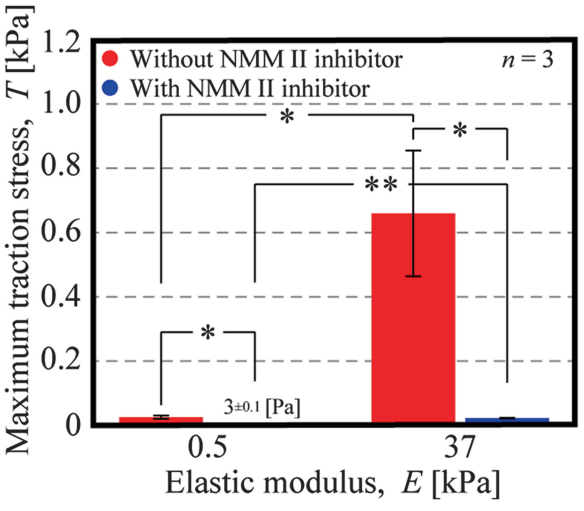


Fig. 2.4 Maximum traction stress, $\boldsymbol{T}$, of hBMSCs in each elastic modulus of the matrix. *Blue* and *red* data represent with and without the NMM II inhibitor, respectively. *n* indicates number of samples. All data are expressed as the means ± SEM. ** $p < 0.01$, * $p < 0.05$

Figure 2.4 shows the maximum cell-induced traction stress in each elastic modulus of the matrix. The maximum traction stress of the cell was dependent upon the elastic modulus of the matrix, and inversely correlated with the displacement trends shown in Fig. 2.3.

The maximum cell-induced traction stress of the respective elastic modulus is shown in blue in Fig. 2.4, when the intracellular NMM II is inhibited. There was big difference in terms of the traction stress values compared to it without NMM II inhibition (shown in red, Fig. 2.4). These results weren't attributable to cytotoxicity of NMM II inhibitor (blebbistantin). The results of the differentiation assessment were shown in Fig. 2.1. There were no clear differences with respect to the morphological evaluation and the gene expression levels in each elastic modulus of the matrix. It says that the cells didn't differentiate into either neurons or osteoblasts. NMM II is one of the vital factors of actin structures in intracellular cytoskeletal dynamics [24]. Furthermore, these actin structures are connected to focal adhesions which provide the pathway of force transmission from inside the cell to elastic matrix [25]. Therefore, it indicates that cytoskeleton plays an important role in mechanical interaction with elastic matrix [26], and acts a key function in cellular differentiation.

2.4 Conclusions

In summary, mechanical fields of elastic matrix and hBMSCs were measured using DVC method to investigate whether the elastic modulus of the matrix determined the differentiation lineage of hBMSCs. The hBMSCs produced large deformation to the matrix when the matrix was soft ($E = 0.5$ kPa) and opposite when the matrix was hard ($E = 37$ kPa). The traction stress of the cell produced, however, became higher when the matrix was hard. Moreover, it suggests that mechanical interaction between elastic matrix and intracellular cytoskeleton is crucial for cellular differentiation. Evaluating the mechanical fields in the mechanical interaction of stem cell differentiation has no precedent and will provide important knowledge in mechanobiology of differentiation.

References

1. Pittenger MF, Mackay AM, Beck SC, Jaiswal RK, Douglas R, Mosca JD, Moorman MA, Simonetti DW, Craig S, and Marshak DR, Science 284, 143–147, (1999)
2. Dominici, M., Le Blanc, K., Mueller, I., Slaper-Cortenbach, I., Marini, F.C., Krause, D.S., Deans, R.J., Keating, A., Prockop, D.J., Horwitz, E.M.: Cytotherapy. **8**, 315–317 (2006)
3. Lazennec, G., Jorgensen, C.: Stem Cells. **26**, 1387–1394 (2008)
4. Morita, Y., Suzuki, S., Ju, Y., Kawase, N.: J Mech Med Biol. **14**, 1450025 (2014)
5. Morita, Y., Watanabe, S., Ju, Y., Xu, B.: Acta Bioeng. Biomech. **15**, 71–79 (2013)
6. Morita, Y., Mukai, T., Ju, Y., Watanabe, S.: Cell Biochem. Biophys. **66**, 73–80 (2013)
7. David, V., Martin, A., Lafage-Proust, H.M., Malaval, L., Peyroche, S., Jones, D.B., Vico, L., Guignandon, A.: Endocrinology. **148**, 2553–2562 (2007)
8. Thorpe, S.D., Buckley, C.T., Vinardell, T., O'Brien, F.J., Campbell, V.A., Kelly, D.J.: Ann. Biomed. Eng. **38**, 2896–2909 (2010)
9. Kratchmarova, I., Blagoev, B., Haack-Sorensen, M., Kassem, M., Mann, M.: Science. **308**, 1472–1477 (2005)

10. Zablotskii, V., Lunov, O., Novotna, B., Churpita, O., Trosan, P., Holan, V., Sykova, E., Dejneka, A., Kubinova, S.: Appl. Phys. Lett. **105**, 103702 (2014)
11. Fan, H.B., Liu, H.F., Toh, S.L., JCH, G.: Biomaterials. **29**, 1017–1027 (2008)
12. Morita, Y., Yamamoto, S., Ju, Y.: Biotechnol. Lett. **37**, 1911–1918 (2015)
13. Khetan, S., Guvendiren, M., Legant, W.R., Cohen, D.M., Chen, C.S., Burdick, J.A.: Nat. Mater. **12**, 458–465 (2013)
14. Chowdhury, F., Na, S., Li, D., Poh, Y.C., Tanaka, T.S., Wang, F., Wang, N.: Nat. Mater. **9**, 82–88 (2010)
15. Engler, A.J., Sen, S., Sweeney, H.L., Discher, D.E.: Cell. **126**, 677–689 (2006)
16. Franck, C., Hong, S., Maskarinec, S.A., Tirrell, D.A., Ravichandran, G.: Exp. Mech. **47**, 427–438 (2007)
17. Vicente-Manzanares, M., Ma, X.F., Adelstein, R.S., Horwitz, A.R.: Nat Rev Mol Cell Bio. **10**, 778–790 (2009)
18. Landau, L.D., Lifshitz, E.M.: Theory of Elasticity. 3rd ed. Sykes, J.B., Reid, W.H. (translators). Pergamon Press, Oxford (1986)
19. Clegg, N., Ferguson, C., True, L.D., Arnold, H., Moorman, A., Quinn, J.E., Vessella, R.L., Nelson, P.S.: Prostate. **55**, 55–64 (2003)
20. Brubaker, K.D., Vessella, R.L., Brown, L.G., Corey, E.: Prostate. **56**, 13–22 (2003)
21. Bay, B.K., Smith, T.S., Fyhrie, D.P., Saad, M.: Exp. Mech. **39**, 217–226 (1999)
22. Maskarinec, S.A., Franck, C., Tirrell, D.A., Ravichandran, G.: P Natl Acad Sci USA. **106**, 22108–22113 (2009)
23. Franck, C., Maskarinec, S.A., Tirrell, D.A., Ravichandran, G.: PLoS One. **6**, e17833 (2011)
24. McBeath, R., Pirone, D.M., Nelson, C.M., Bhadriraju, K., Chen, C.S.: Dev. Cell. **6**, 483–495 (2004)
25. Tamada, M., Sheetz, M.P., Sawada, Y.: Dev. Cell. **6**, 709–718 (2004)
26. Mathieu, P.S., Loboa, E.G.: Tissue Eng B. **18**, 436–444 (2012)

http://www.springer.com/978-3-319-63551-4

Mechanics of Biological Systems, Materials and other topics in Experimental and Applied Mechanics, Volume 4

Proceedings of the 2017 Annual Conference on Experimental and Applied Mechanics

Zavattieri, P.; Minary, M.; Grady, M.E.; Dannemann, K.; Crone, W. (Eds.)

2018, VII, 100 p. 111 illus., 82 illus. in color., Hardcover
ISBN: 978-3-319-63551-4